Fracture Prediction of High Strength Steels with Ductile Fracture Criterion and Strain Dependent Model of Anisotropy

Kenji Takada* , Kentaro Sato** , Ninshu Ma***

*Honda R&D Co.,Ltd. Automobile R&D center, 4630 Shimotakanezawa, Haga-machi,Haga-gun, Tochigi, 321-3393, Japan

**JFE Steel Corporation, 1 Kawasaki-cho,Chuo-ku,Chiba 260-0835, Japan

***JSOL Corporation, 2-2-4 Tosabori,Nishi-ku,Osaka 550-0001,Japan

Abstract

Cockcroft-Latham fracture criterion was applied to predict the fracture of high strength steels. Marciniak-type biaxial stretching tests of the four grades of high strength steels were carried out to measure the material constant of Cockcroft-Latham fracture criterion. Furthermore, in order to improve the simulation accuracy, the local anisotropic parameters depending on the plastic strain (strain dependent model of anisotropy) were measured by Digital Image Reconstruction system and incorporated into Hill's anisotropic yield condition by authors. To confirm the validity of Cockcroft-Latham fracture criterion, the uniaxial tensile tests based on JIS No.5 tensile specimen were performed. The force-displacement history and fracture happening strokes were predicted with high accuracy. Then, Cockcroft-Latham fracture criterion was applied to predict the failure of four types of spot welded joints. To simulate the local bending and warping deformations around the heat-affected zone, the discrete Kirchhoff triangle element was adapted. FEM results for four grades of high strength steels and four types of spot welded joints had good correlation with experimental ones.

Introduction

In order to reduce the automobile body weight and to improve the crashworthiness, the use of high strength steels is greatly increasing these years. However, the high strength steels become less ductile in general. The fracture of steel material and spot weld failure may occur due to local deformation. Therefore, in finite element analysis, the accuracy improvement of fracture prediction is greatly required by automotive industries. In this study, Cockcroft and Latham fracture criterion was employed to predict the fracture of high strength steel sheets and the failure around the spot welds [1-3]. In order to obtain

the material constants of Cockcroft and Latham fracture criterion, the Marciniak-type in-plane biaxial stretching test was carried out for four classes of high strength steels. Then fracture strains and material fracture constants were determined using the measured data at plane strain state. Furthermore, to reproduce the local fracture behaviors, the local anisotropic r-value (ratio of local width strain to local thickness strain) which depends on the local plastic strain, was accurately measured using Digital Image Reconstruction system. The strain dependency of local anisotropic r-value, named as the strain dependent model of anisotropy was proposed in this study and was incorporated into Hill's anisotropic yield condition. In order to confirm the validity of Cockcroft-Latham fracture criterion, the uniaxial tensile tests based on JIS No.5 tensile specimen were performed. It was found that the accuracy of predicted rupture strokes was greatly improved if the strain dependent model of anisotropy is employed. Then, Cockcroft-Latham fracture criterion was adapted to the prediction of failure of spot welds. In order to consider the local bending and warping around the nugget, the discrete Kirchhoff triangle element was applied and this modeling got the good correlation with experimental results.

Cockcroft-Latham ductile fracture criterion[4]

Cockcroft-Latham fracture criterion showing in Eq. (1) is the integral damage value using the maximum principle stress and equivalent strain. It needs only one material constant to express the amount of ductile damage. Therefore material constant can be determined only by one experiment.

$$\int_0^{\bar{\varepsilon}_f} \sigma_{\max} d\bar{\varepsilon} = C_1 \qquad (1)$$

where, σ_{max} is the maximum principle stress, $\bar{\varepsilon}$ is the equivalent strain, $\bar{\varepsilon}_f$ is the equivalent strain at which the fracture occurs, C_1 is the material constant to express the limit of ductile damage. The integral I showing in Eq.(2) is the normalized damage value of Eq.(1). This integral I is calculated at each integration points (Gauss points), using the stresses and strains computed by finite element analysis. If the integral I at Gauss point of an element becomes 1, its damage value in the element reaches the fracture criterion and element is deleted.

$$I = \frac{1}{C_1} \int_0^{\bar{\varepsilon}_f} \sigma_{\max} d\bar{\varepsilon} \qquad (2)$$

Marciniak-type in-plane biaxial stretching test

Marciniak-type in-plane biaxial stretching test was carried out in order to measure the material constant C_1 and rupture strain $\bar{\varepsilon_f}$ showing in Eq.(2). The high strength steels used in this study were 440MPa grade, 780MPa grade , 980MPa grade with a thickness of 1.2mm and 1180MPa grade with a thickness of 1.4mm. In the test specimen, the scribed lattice lines with 2mm pitches were printed to measure the fracture strain. If Cockcroft-Latham fracture criterion is expressed in strain space, it is proven that strain limit of ductile fracture becomes the straight line showing in Fig.(1)[1,2]. In other words, the strain limit of ductile fracture can be determined only by one experiment in which strain ratio($\beta = \varepsilon_2/\varepsilon_1$) is 0. Therefore, in this study, Marciniak-type test was carried out only at the plane strain state. Table.1 shows the anisotropic r-values and material constants for four classes of high strength steels. The anisotropic r-values shown in Table.1 were obtained by conventional method in which the strains are measured by extensometer with large gauge length.

Example of Marciniak test

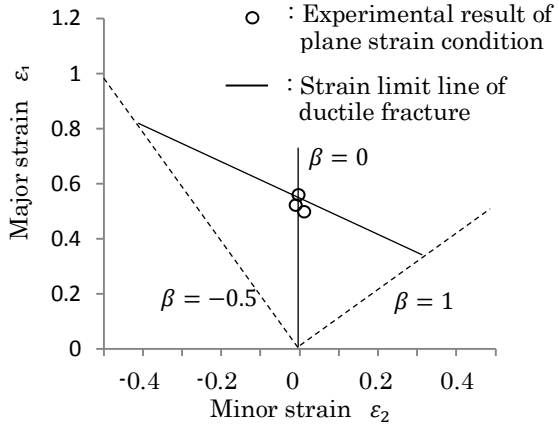

Fig.1 Example of limit strain for fracture in biaxial stretching tests

Table 1. Tensile properties of high strength steels

Material grade	440MPa	780MPa	980MPa	1180MPa
Gauge length [mm]	50	50	50	50
Prestrain [%]	10	12	5	4
r- value : r (C direction)	1.0	0.87	0.92	0.86
Material constant : C_1	484	691	612	579

Finite Element Analysis (FEA)

The uniaxial tensile tests based on JIS No.5 tensile specimen were carried out to investigate the Cockcroft-Latham fracture criterion. A general purpose nonlinear FE code LS-DYNA ver.971[5] and user subroutine including Cockcroft-Latham fracture criteria developed by JSOL [3] were used for the simulations. Hill's 48 anisotropic material model was selected in simulation. The stress-strain relations for high strength steels were defined by load curves.

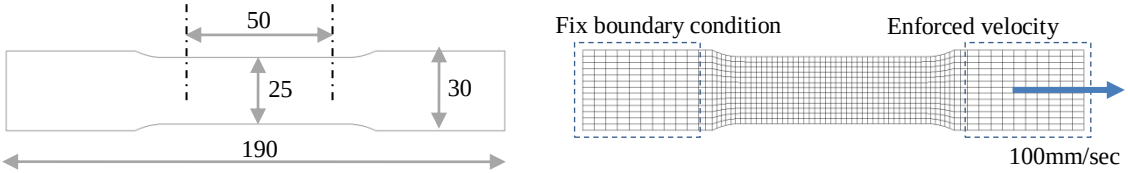

Fig.2 Dimensions of the uniaxial tensile test and finite element model of LS-DYNA

The uniaxial tensile test specimen was modeled with Belytschko-Tsay element having 5 integration points along the thickness. The element size of fracture area is 2mm x 2mm which is similar to scribed lattice lines of Marciniak test and enforced velocity was applied parallel to the X axis showing in Fig.2.

Fig.3 shows the Force-Stroke curves of experimental and LS-DYNA results. As to the 440MPa and 780MPa grade, the maximum forces and rupture strokes had good correlations with experimental results. On the other hand, as to the 980MPa and 1180MPa grade, the rupture strokes of simulation results were longer than experimental. In the case that power-law hardening rule is used, diffuse necking occurs at work hardening exponent (n-value) and localized necking occurs at about twice of n-value (2n) and finally material is ruptured. However from the results shown in Figs.3 (c) and (d), it was found that rupture of 980MPa and 1180MPa grade occurred immediately after diffuse necking.

In the FEA, the conventional anisotropic r-values shown in Table.1 were employed. And these anisotropic r-values were constant values up to rupture. However, the measured results had shown that the local anisotropic r-values of 980MPa and 1180MPa grades decrease immediately after n-value. The strain dependency of anisotropic r-value was also observed by other researchers [6,7]. However, the subject of strain dependency is up to n-value at which the uniform elongation finishes. There are no papers investigating the phenomenon after n-value. Therefore, in this study, the local anisotropic r-value was measured using Digital Image Reconstruction system.

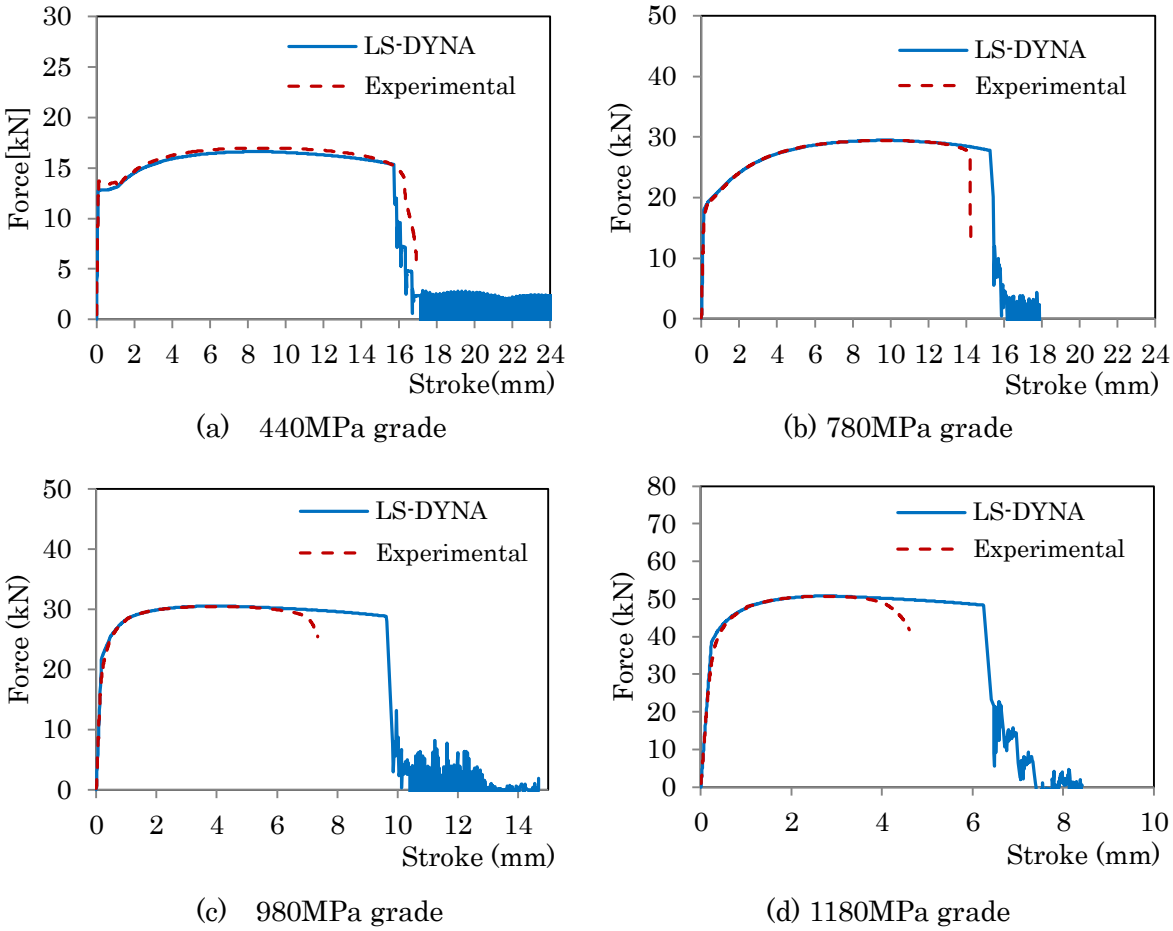

Fig.3 Comparison between experimental and FEM results with fixed anisotropic r-value

Digital Image Reconstruction system

Digital Image Reconstruction system (in-house system of JFE steel) was applied to measure the local anisotropic r-value as a function of tensile strain as shown in Fig.4. The geometry of specimen was based on JIS No.5 tensile specimen and it was prepared with grid points with 1mm pitch. The three digital cameras were set up near the specimen and took pictures for fixed interval. After testing, digital images were analyzed using software to calculate the major and minor strains. And the strain at the thickness direction was calculated using constant volume rule. Fig.5 and Fig.6 show the local anisotropic r-values (ratio of local width strain to local thickness strain) of 980MPa grade and 1180MPa grade using Digital Image Reconstruction system. In the 980MPa grade, the conventional anisotropic r-value was 0.92 (Table.1). While, the local anisotropic r-value was about 0.75 up to uniform elongation (n-value) and its value decreased gradually after n-value. As to the 1180MPa grade, the conventional

anisotropic r-value was 0.86 (Table.1). While, the local anisotropic r-value was about 0.75 and decreased greatly after n-value.

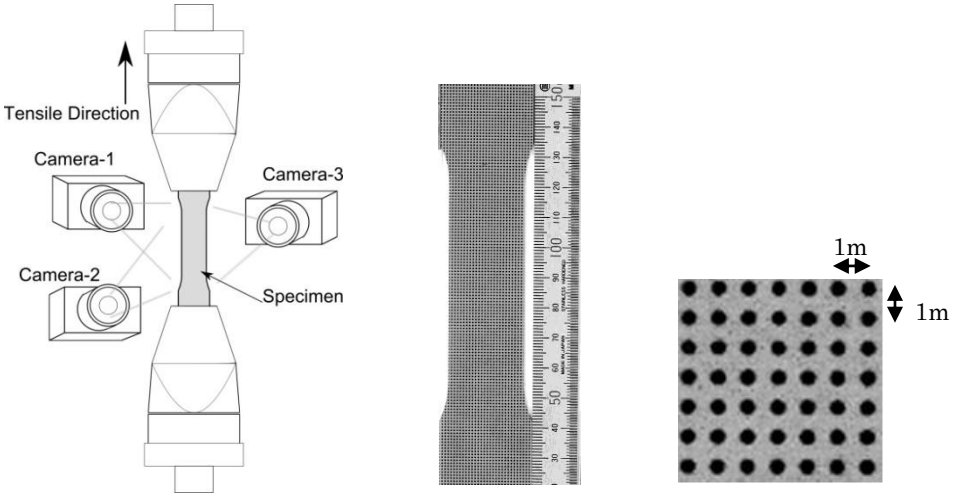

(a) Measurement System (b) Specimen with grid (c) Grid pitch : 1mm x 1mm

Fig.4 Digital Image Reconstruction system

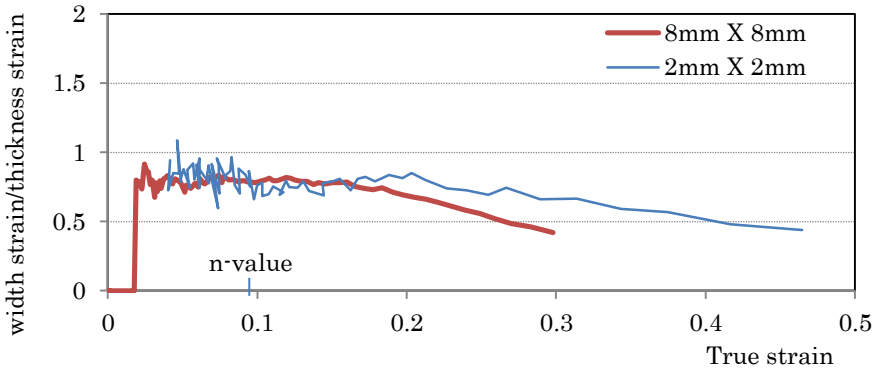

Fig.5 Local anisotropic r-value (width strain/thickness strain) of 980MPa grade

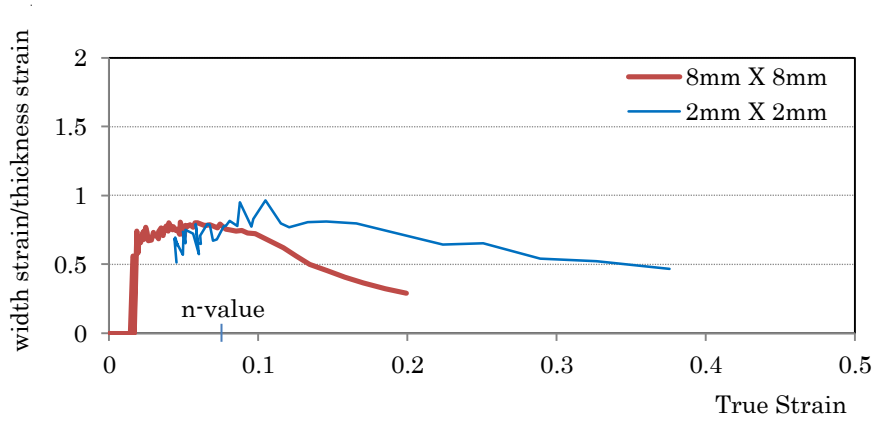

Fig.6 Local anisotropic r-value (width strain/thickness strain) of 1180MPa grade

Improvement of existing yield condition with strain dependent model of anisotropy

There are several yield functions for anisotropic materials. In present study, Hill's anisotropic yield condition well used for steel materials was selected as shown in Eq.(3) and Eq.(4). The strain dependent model of the local anisotropic r-value was incorporated into this Hill's anisotropic yield condition by authors. In other words, in order to deal with the strain dependency of the local anisotropic r-values, H, G, F and N were modified as shown in Eq.(5).

$$\sqrt{F(\sigma_y-\sigma_z)^2+G(\sigma_z-\sigma_x)^2+H(\sigma_x-\sigma_y)^2+2N\sigma_{xy}^2+2L\sigma_{yz}^2+2M\sigma_{zx}^2}=\sigma_Y(\bar{\varepsilon}^p) \quad (3)$$

$$\left.\begin{aligned} H&=\frac{R_{00}}{1+R_{00}},\ G=\frac{H}{R_{00}}=\frac{1}{1+R_{00}},\ F=\frac{H}{R_{90}}=\frac{R_{00}}{(1+R_{00})R_{90}} \\ N&=(R_{45}+1/2)(F+G)=\frac{(1+2R_{45})(R_{00}+R_{90})}{2(1+R_{00})R_{90}} \end{aligned}\right] \quad (4)$$

$$\left.\begin{aligned} H&=\frac{R_{00}(\bar{\varepsilon}^p)}{1+R_{00}(\bar{\varepsilon}^p)},\ G=\frac{H}{R_{00}(\bar{\varepsilon}^p)}=\frac{1}{1+R_{00}(\bar{\varepsilon}^p)},\ F=\frac{H}{R_{90}(\bar{\varepsilon}^p)}=\frac{R_{00}(\bar{\varepsilon}^p)}{(1+R_{00}(\bar{\varepsilon}^p))R_{90}(\bar{\varepsilon}^p)} \\ N&=(R_{45}(\bar{\varepsilon}^p)+1/2)(F+G)=\frac{(1+2R_{45}(\bar{\varepsilon}^p))(R_{00}(\bar{\varepsilon}^p)+R_{90}(\bar{\varepsilon}^p))}{2(1+R_{00}(\bar{\varepsilon}^p))R_{90}(\bar{\varepsilon}^p)} \end{aligned}\right] \quad (5)$$

Fig.7 shows the simulation results considering the local anisotropic r-value. It was found that accuracy of rupture strokes for ultra high strength steels was greatly improved.

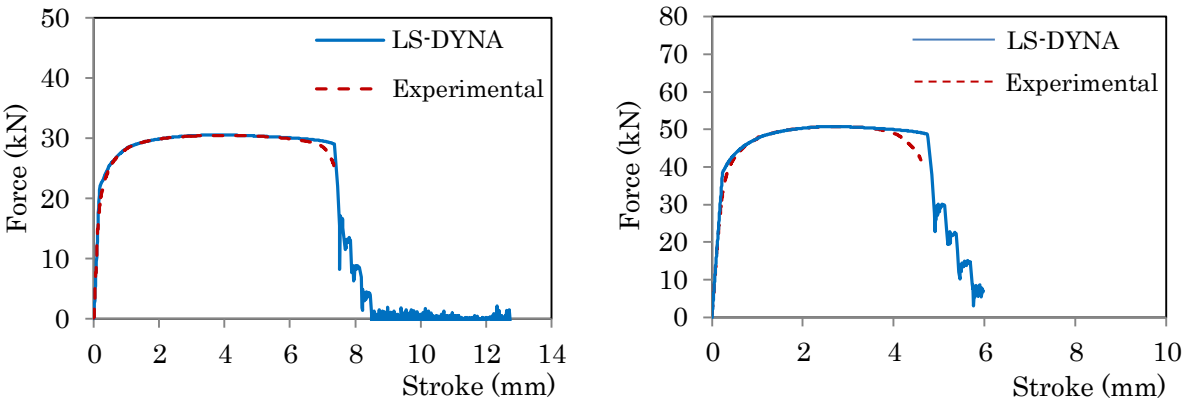

(a) 980MPa grade (b) 1180MPa grade

Fig.7 Comparison between experimental and FEM with the local anisotropic r-value

Investigation of equivalent plastic strain

The equivalent plastic strain at which the fracture occurred was investigated using the result of 980MPa grade steel. The Fig.8 shows the fracture locus in the JIS No.5 tensile specimen. While, Fig.9 shows the equivalent plastic strain-time curves at the fracture locus. In the case of simulation result considering the local anisotropic r-value, the equivalent plastic strain was increased from about 0.06sec. Therefore, the rupture stroke of simulation result with the local anisotropic r-value was decreased.

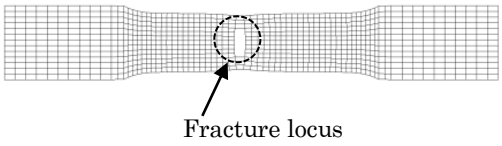

Fig.8 Fracture locus of 980MPa grade in JIS No.5 tensile specimen

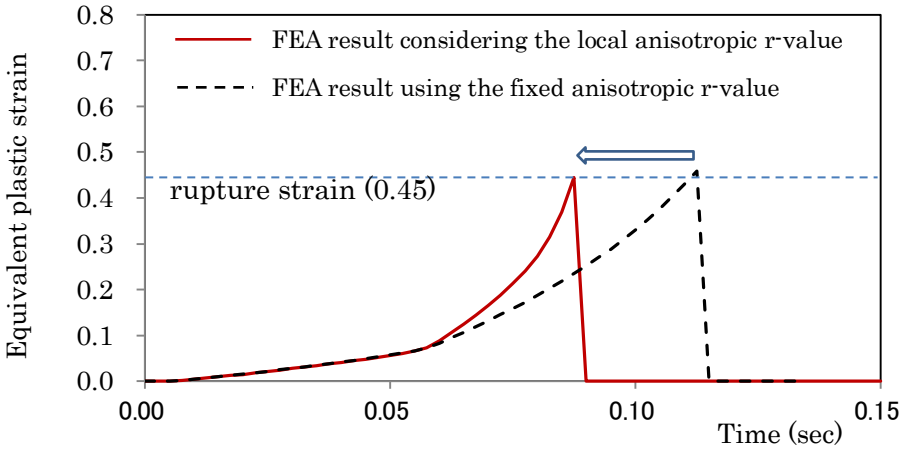

Fig.9 Equivalent plastic strain – time curves in fracture locus

Application to spot weld failure

Cockcroft-Latham fracture criterion was applied to spot weld failure to predict the bending and warping deformation. In general, the failure modes of spot welds are classified into three types. In the Fig.10, (a) is the fracture of steel material around the heat-affected zone (HAZ), (b) is fracture at HAZ, and (c) is interfacial failure. In this study, Cockcroft-Latham fracture criterion was applied to (a) and (b). The four kinds of joint test were carried out to investigate the accuracy showing in Fig.11 [8,9]. They were named as DS-joint, TS-joint, LT-joint and UT-joint respectively.

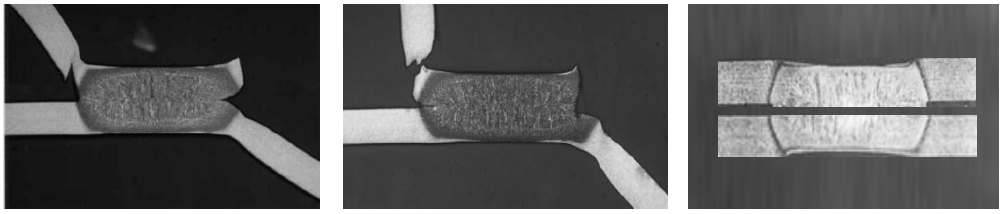

(a) plug fracture (b) HAZ fracture (c) interface fracture

Fig.10 Classification of failure of spot welds

(a) DS-joint (b) TS-joint (c) LT-joint (d) UT-joint

Fig.11 Specification of specimen

The high strength steels used in this study were 440MPa grade and 590MPa grade with a thickness of 1.2mm. Table.2 shows the material properties.

Table 2. Mechanical properties of 440MPa and 590MPa grade steels

	YS(MPa)	TS(MPa)	EL(%)	Thickness(mm)	Surface	C_1
440MPa	335	460	35.2	1.2	Uncoated	484
590MPa	427	659	25.5	1.2	Uncoated	340

Finite Element Simulation

In the LT-joint and UT-joint, the strong local bending and warping deformation occur around HAZ by the external tensile force. If quadratic elements with C1 continuous shape function are applied, local bending and warping may be calculated. However, generally, quadratic elements are expensive for CPU time. So, in this study, discrete Kirchhoff triangle element (DKT element) of LS-DYNA was applied. The effectiveness of DKT element was proven by Batoz and Bathe[10]. And comprehensive analytical study of DKT element was performed by Wu, Li and Belytschko[11]. The use of DKT element is shown in Fig.12. Basically, L-joint specimen was consisted by Belytschko-Tsay elements and the DKT elements with 5 integration point along the thickness were set up the around HAZ area only.

Fig.13 shows the force-stroke curves. By the DKT elements, simulation results had good correlation with experimental. Fig.14 shows deformed modes of four kind joint models. From these results, it was recognized that Cockcroft and Latham fracture

criterion is able to simulate the local bending and warping deformation.

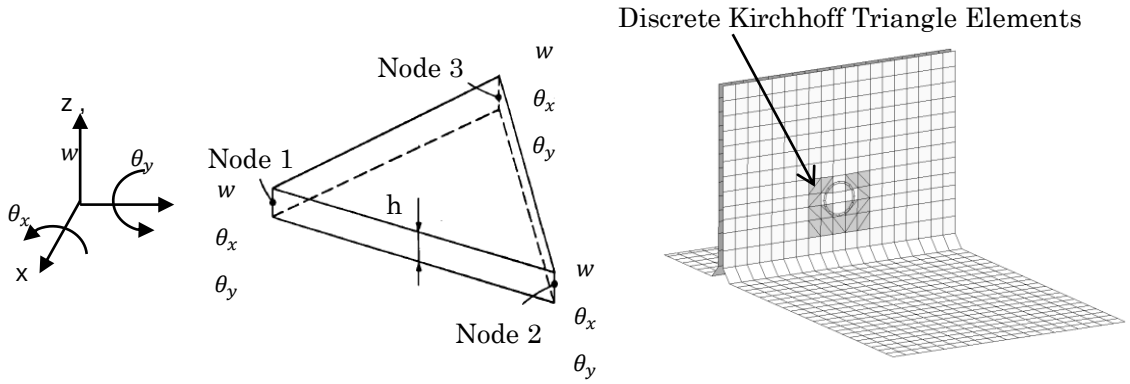

Fig.12 FE model of LT-joint with Discrete Kirchhoff Triangle Elements

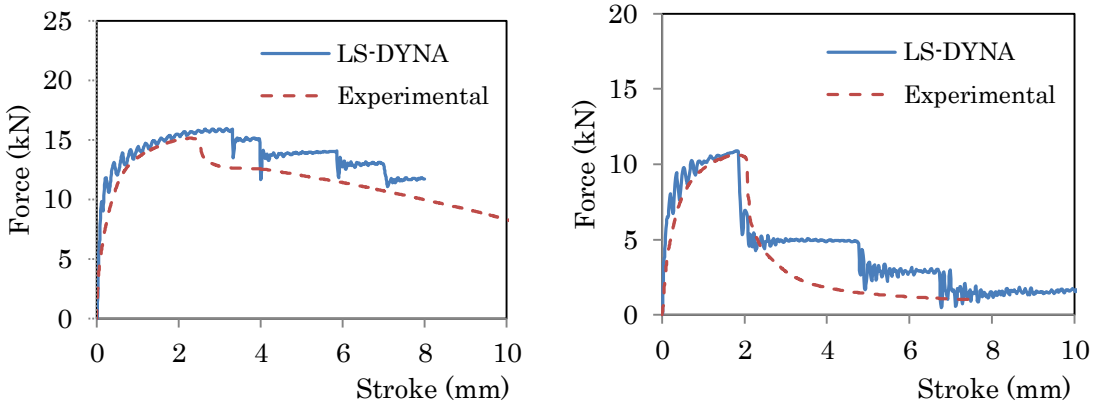

(a) DS-joint (b) TS-joint

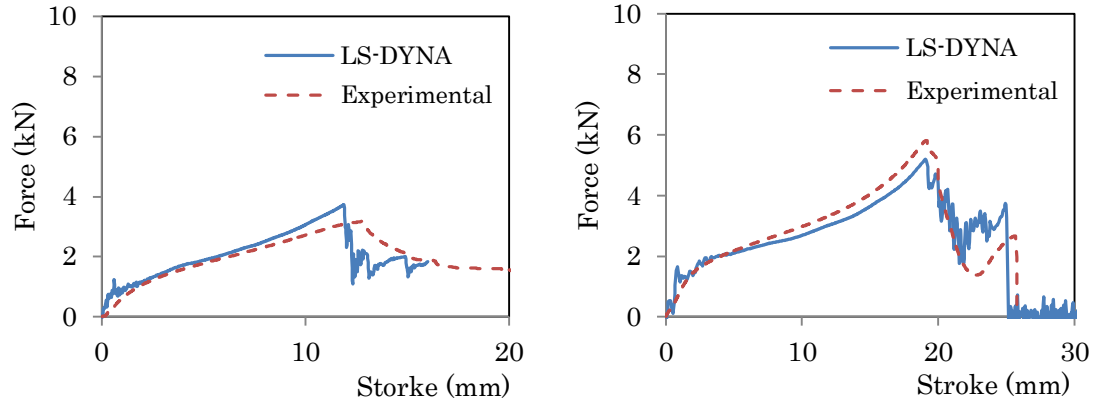

(c) LT-joint (d) UT-joint

Fig.13 Force-stroke curves of 440MPa grade steel

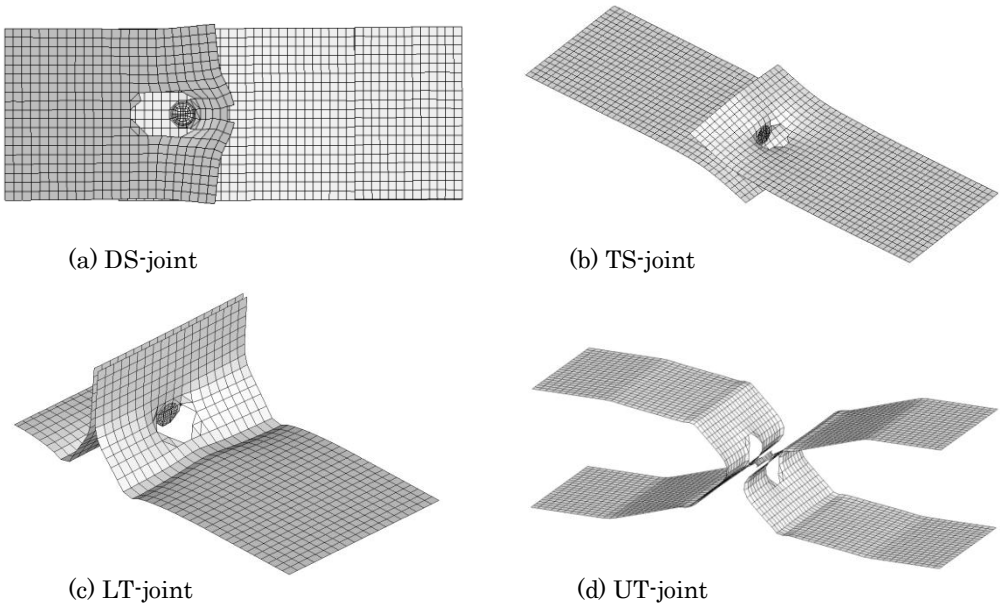

(a) DS-joint (b) TS-joint

(c) LT-joint (d) UT-joint

Fig.14 Deformation modes of four kinds of spot weld models of 440MPa grade

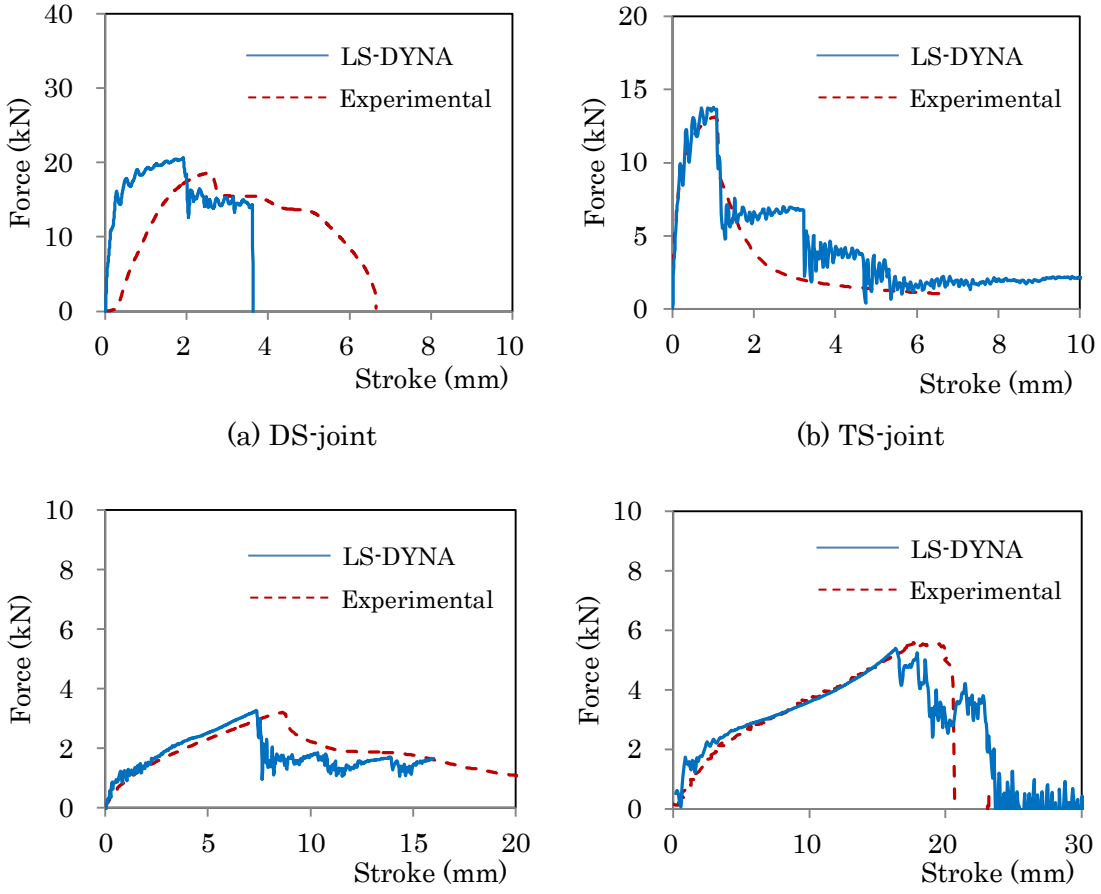

(a) DS-joint (b) TS-joint

(c) LT-joint (d) UT-joint

Fig.15 Force-stroke curves of 590MPa grade steel

Fig.15 shows the force-stroke curves of 590MPa grade. As to the DS-joint, chuck of the tensile testing machine slipped. However, the maximum forces of simulation result had good correlation with experimental. In the 590MPa grade steel, failure occurred in HAZ and rupture strain decreased. So, in this case, material constant C_1 of Cockcroft-Latham fracture criterion was revised.

Conclusions

In this study, Cockcroft-Latham fracture criterion was applied to predict the fracture of high strength steels and failure of spot welds. Using the Digital Image Reconstruction system, the local anisotropic r-values were measured and these characteristics were incorporated into Hill's anisotropic yield condition. As a result, the rupture strokes of ultra high strength steels of 980MPa and 1180MPa grades had good correlation with experimental. As to the failure of spot welds, it was found that DTK element was useful to predict the local bending and warping around HAZ.

Acknowledgement

The authors thank Prof. H. Takuda from Department of Energy Science and Technology of the Kyoto University for valuable comments.

Reference

[1] Takuda H., Kanie T., Isogai E., Yoshida T., : Finite Element Analysis of Forming Limit of High-strength Steel Sheets Using Ductile Fracture Criterion, Tetsu-to-Hagane, Vol.91 (2005) No.6

[2] Takuda H., Hama T., Nishida K., Yoshida T., Nitta J. : Prediction of Forming Limit in Stretch Flanging by Finite Element Simulation Combined with Ductile Fracture Criterion, Computer Methods in Materials Science, Vol.9, 2009, No.1

[3] Ma N., Umezu Y., Watanabe Y.,: Development and Applications of Simulation System JSTAMP/NV for Tube Hydro-Forming,CP908,NUMIFORM'07 (2007)

[4] Cockcroft M., G., Latham D. J. : Ductility and the Workability of Metals, Int. J. Met. 96(1968)

[5] JSOL：LS-DYNA Keyword User's Manual Volume I Version971 (2007)

[6] Huang G., Yan B., Xia Z.：Measurement of r-values of High Strength Steels Using Digital Image Correlation, SAE Technical Paper 2011-01-0234, (2011)

[7] Kawai N., Hayashi N., Murata Y., Iwata H., Kurita M.：Variations of r Value and Texture for Mild Steel and Commercially Pure Aluminum Sheet Prestrained in Uniaxial Tension, Journal of JSTP ,No.32-365 (1991)

[8] Utsumi Y., Sato K., Nomura N., Suganuma H., Takada K., etc：Investigation and Research into CAE Technique for Spot Weld Rupture (Part I), JSAE, No.49-05 (2005)

[9] Yamamoto M., Inoue T., Utsumi Y., Kanamori M., Kobayashi T., etc：Investigation and Research into CAE Technique for Spot Weld Rupture (Part V),JSAE, No.49-05 (2005)

[10] Batoz J.L., Bathe K.J, Ho L.W.,：A Study of Three-Noded Triangular Plate Bending Elements, International Journal for Numerical Methods in Engineering, Vol.15, 1771-1812 (1980)

[11] Wu S., Li G., Belytschko T.：A DKT shell element for dynamic large deformation analysis, Communications in Numerical Methods in Engineering, Vol21, p.651-675 (2005)